Use of Concrete Cross Walls to Reduce Movements Induced by Deep Excavation

**Chang-Yu Ou[1], Pio-Go Hsieh[2] and Shao-Chi Chien[3]*

[1] *Department of Construction Engineering, NTUST, Taipei 10672, Taiwan*
[2] *Department of Assets and Property Management, HWH, New Taipei City 23568, Taiwan*
[3] *Department of Information Tourism, AU, New Taipei City 25103*, Taiwan
[1] *ou@mail.ntust.edu.tw*

ABSTRACT

In this study, an excavation case history, installed with cross walls case history, is presented. A three-dimensional numerical analysis for the excavation with cross walls was introduced. Both the observed and computed wall deflections for the studied case history were studied to demonstrate the effectiveness of cross walls in reducing lateral wall deflection induced by deep excavation. Results show that the maximum lateral wall deflection can be reduced by 77% at the cross wall section and 72% at the midpoint between two cross walls. A series of parametric study was performed to study the effect of cross wall depth on the lateral wall deflection. It is found that installation of the full cross wall depth can result in the best reduction in the lateral wall deflection. However, use of the cross wall height of 0.4~0.6 times the excavation depth and concrete cross wall embedment of 0.5~0.7 times the embedded diaphragm wall depth can yield the lateral wall deflection very close to that of full concrete cross wall depth.

1. INTRODUCTION

Since the density of buildings in urban areas in Taiwan is relatively high, deep excavations are often conducted next to buildings or public facilities. Necessary auxiliary measures are normally required to avoid the damage of adjacent buildings. Cross walls are common construction methods used in Taiwan for protection of adjacent buildings during excavation. The cross wall is built with concrete in an

---

excavation transversely before excavation, as shown in Fig. 1, using the same diaphragm wall construction technique, e.g., construction of guided walls, excavation of trench, casting of concrete and so on. Both ends of cross walls are connected with two opposite diaphragm walls. The function of cross walls in mechanism is similar to a lateral strut, but the cross wall exists before excavation. Because of the high compressive strength and stiffness of cross walls, it is expected to reduce the lateral wall deflection and ground settlement during deep excavation.
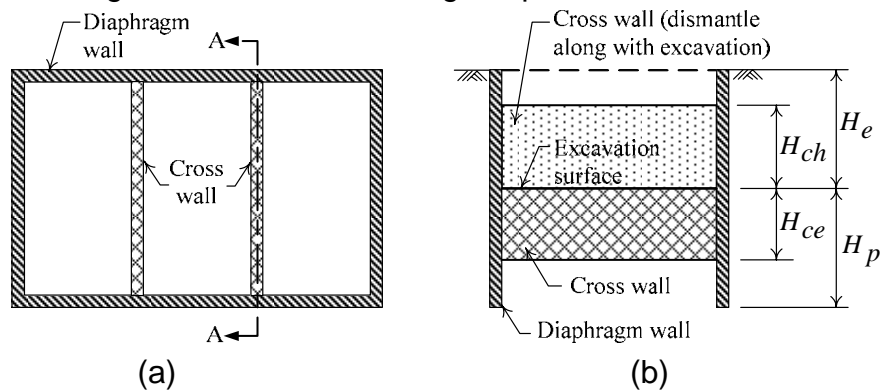

Fig. 1. Schematic diagram of the cross wall (a) plan and (b) section A-A.

Though cross walls have been used in some excavations in Taiwan, studying on cross wall behavior is few and even documented case histories are rare. Current designs mostly remain in accordance with experiences, and the effect of reducing lateral wall deflection has not yet been verified. Moreover, cross walls can be constructed with full depth, that is, from the ground surface down to the bottom of the diaphragm wall or with partial depth, namely, from a certain depth below the ground surface down to a depth below the excavation surface. Therefore, a further study of allocations of cross walls on the reduction of lateral wall deflection is necessary.

In this study, a case history with good monitoring results is presented. A reasonable three-dimensional numerical analysis for the excavation with cross walls was introduced. Both the observed and computed lateral wall deflections for the studied case history were compared. Moreover, the same excavation but with the assumption that no cross walls were installed was analyzed to demonstrate the effectiveness of cross walls in reducing lateral wall deflection induced by excavation.

Finally, a series of parametric studies on the different depths of cross walls are performed using the three-dimensional numerical method to examine the influence of cross walls in reducing the lateral wall deflection. It is expected that with more understanding the effect of cross wall depth in reducing the lateral wall deflection, cross walls in excavations can be designed in a more compact way and to ensure the protection of adjacent buildings.

2. THE CASE HISTORY

2.1. Project overview

The case, situated in the Sinyi district of the Taipei city, is a 30-story structure with a seven-level basement. The excavation site was about 121.8 m long and 66.1 m wide. Fig. 2 shows the plan view (Ou 2006, Ou 2011). No buildings existed near the

excavation. The diaphragm wall, designed with 27.5 MPa of the compressive strength (f'_c), was 1.5 m in thickness, and extended from ground surface down to a depth of 57.5 m, about 6.5 m penetrating into the silty sand /gravel formation. The excavation depth was 32.5 m, which was completed using the top-down construction method with seven levels of concrete slab as shown in Fig. 3. The concrete slabs 1FL and B1FL used the beam-plate system, which had thicknesses of 25 cm and 20 cm, respectively; the concrete slabs B2FL~B6FL used the flat slab system, which had a thickness of 61 cm. After excavating down to GL-29.4 m (GL refers to the ground surface level), 3-H400x400x13x21 mm steel struts, with a spacing of 6.4 m and slope of 4.6:6, were installed as temporary supports. The site was then excavated to GL-32.5 m.
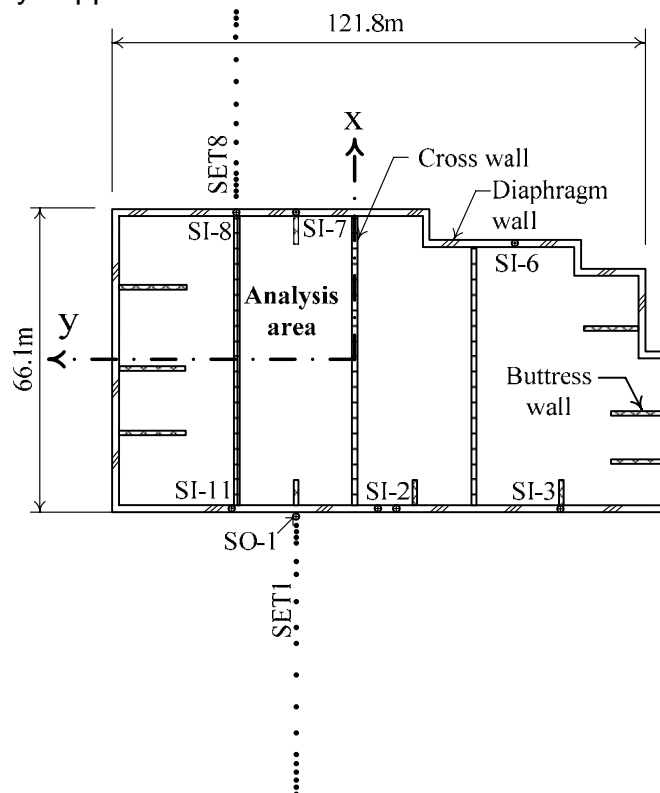

Fig. 2. Plan view and the instrumentation of the case history.

To reduce the lateral wall deflection and ground settlement induced by excavation, 3 cross walls of 1.0 m in thickness and 26 m in intervals (L') were constructed and their depths were between GL-1.5 m and GL-45m in the north-south direction. Ten buttress walls of 1.0 m thickness and 55 m depth, with lengths varying from 6 m to 15 m, were constructed where relatively large lateral wall deflection was expected (Fig. 2). The cross walls and buttress walls between GL+0 m to GL-1.5 m were backfilled with the in-situ soil, those between GL-1.5 m to GL-22 m were cast with 13.7 MPa concrete, and those below GL-22 m were cast with 24.0 MPa concrete. Both the cross wall and buttress wall were demolished with excavation process.

Many inclinometers were installed along the excavation sides. The inclinometers SI-8 and SO-1 and their corresponding settlement measurement sections, SET8 and SET1, were used to compare with analysis results (Fig. 2). The complete field observation data for this project are shown in Ou (2006).

2.2. Subsurface soil profile

The bedrock is located at a depth of 66.7 m, and its SPT-N value is greater than 50. Above the bedrock are silty clay (CL) and silty sand with gravel (SM/GW). The groundwater table is located at GL-3 m. The porewater pressure in silty clay is generally hydrostatic, but the piezometric porewater pressure in the SM/GW was 10 m below the ground surface, i.e., at GL-10 m. The total unit weight (γ_t), effective internal friction angle (ϕ'), over-consolidation ratio (OCR), SPT-N value, undrained shear strength (s_u) and porewater pressure (u_w) are shown in Fig. 4. As shown in the figure, the undrained shear strength of clay was obtained from the triaxial unconsolidated undrained (UU) test and the effective strength parameters for clay and sand/gravel were obtained from triaxial consolidated undrained test and the direct shear test, respectively.
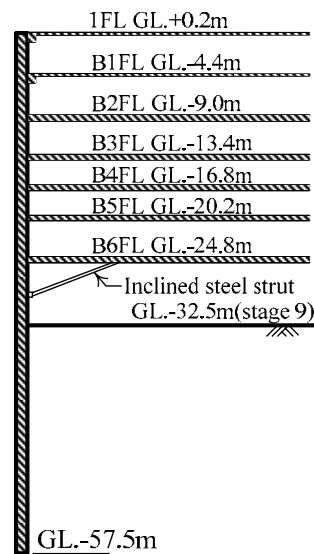

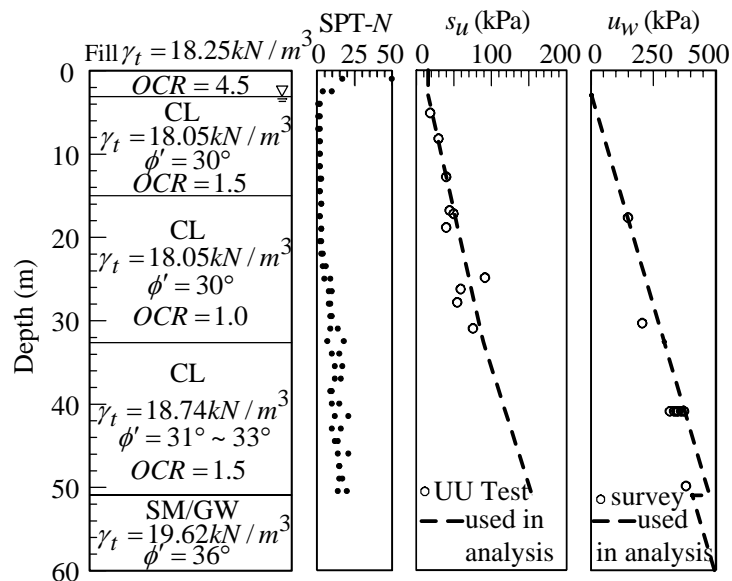Fig. 3. Locations of the slabs and steel strut for the case history.

Fig. 4. The subsurface soil layers for case history.

1965

2.3. Monitoring results

The relationship between the maximum wall deflections and excavation depths for excavations in soft clay in Taipei, under the plane strain condition and without remedial measures like soil improvement, has been studied by Ou (1993), as shown in Fig. 5. As shown in this figure, the maximum wall deflection (δ_{hm}) increases with the excavation depth (H). The wall deflection in soft clay is generally greater than that in sand. The ratio of the maximum wall deflection to excavation depth (δ_{hm}/H) is around 0.2% to 0.5%, in which the upper limit is mostly for clay, the lower limit for sand and those for the alternating layers of sand and clay fall in between the two limits. This figure represents general trend of wall deflections for excavations in Taipei. Fig. 5 also presents the maximum wall deflections obtained from the 8 inclinometers in the north-south direction at the final stage in this case history. Because the case was situated in clayey layer, the relationship should be close to upper limit. However, the observed results are actually below and near the lower limit, much smaller than those of the excavations with similar depths in Taipei (Ou 1993), also much smaller than those of the cases compiled by Clough (1990).
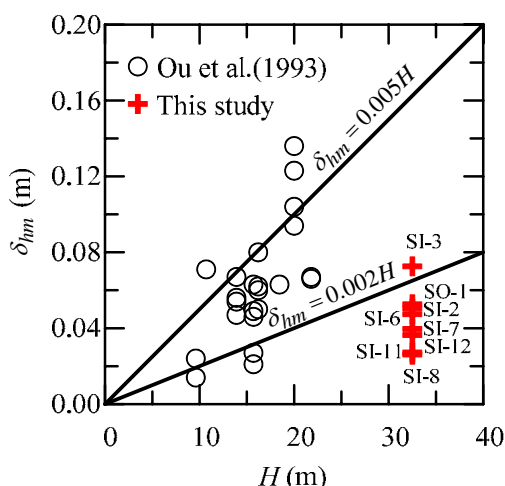

Fig. 5. Relationship between the maximum wall deflection and excavation depth.

Fig. 6 shows the lateral wall deflection and ground settlement at the final stage of excavation at SI-8 (SET8), which was located at the section where the cross wall was installed. As shown in this figure, the wall deflection was extremely small, and the maximum wall deflection reached barely 2.61cm. The wall displayed a concave type of displacement, in which the maximum wall deflection occurs near the excavation surface while the wall below the excavation surface showed a linear type of displacement because of the restraining effect of the cross wall. The ground settlements were also comparatively small, with a maximum value reaching 1.2 cm. As shown in Fig. 6, the δ_{hm}/H was equal to 0.08%, much less the lower limit of the general trend for deep excavations in Taipei. This implies that the cross wall has a significant effect in reducing wall deflection and ground settlement.

Fig. 6 also shows the lateral wall deflections and ground settlement at the final stage of excavation at SO-1 (SET1) section, located at the midpoint between two cross walls. As shown in this figure, the wall deflection and the ground settlement were of the larger

magnitude than those at the SI-8 (SET8) section. The δ_{hm} was 4.74 cm. The ground settlement was also very small, with a maximum value being 1.34 cm. As shown in Fig. 6, the δ_{hm}/H was equal to 0.14%, which is also less than the lower limit of the general trend.
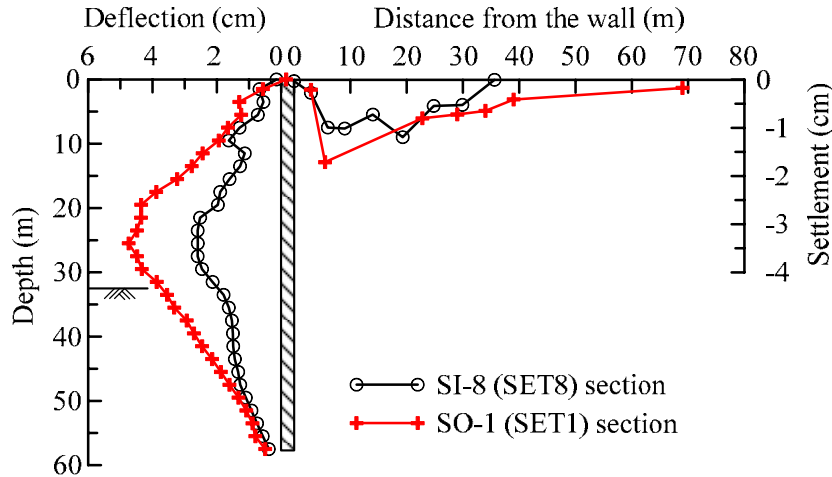

Fig. 6. The observed wall deflections and ground surface settlements at the final excavation stage for SI-8 (SET8) and SO-1 (SET1) sections.

3 NUMERICAL ANALYSIS

3.1. Parameters and mesh

A three-dimensional finite difference computer program, FLAC^{3D} (Itasca Consulting Group, Inc. 1997), is used as a basic numerical analysis tool. A pressure dependent linear elastic-perfectly plastic constitutive model with the plasticity plateau described by the Mohr-Coulomb strength criterion is adopted to simulate the behavior of both clay and sand. Table 1 lists the parameters used for analysis where the coefficient of earth pressure at rest (K_0) was obtained according to Jaky (1944) and Alpan (1967); the normalized undrained Young's modulus (E_s/s$_u$, E_s is Young's modulus) for the Taipei silty clay was found around 400 (Lim 2010), and Poisson's ratio (ν) for clay under the undrained condition can be set equal to 0.495. For typical sand, it is normally assumed that ν =0.3. Considering that the E_s of sand increases with the confining pressure, the E_s can be estimated according to Janbu (1963)

$$E_s = KP_a\left(\frac{\sigma'_3}{P_a}\right)^n,$$

(1)

where P_a is the atmospheric pressure, K is the stiffness modulus number, and n is the stiffness modulus exponent and σ'_3 is the minor effective principal stress.
According to Ou (1994), n can be reasonably assumed to be 0.5. K can be estimated by the wave equation, in which the shear wave velocity of soil can be obtained from the cross-hole test or estimated by the relationship between the shear wave velocity and SPT-N value.

Table 1. Input soil parameters for numerical analysis.

(a) Parameters for clay

Depth (m)	γ_t (kN/m^3)	K_0	s_u* (kPa)	E_s / s_u	ν
0~3.0	18.25	0.93	16	400	0.495
3.0~15.0	18.05	0.59	16~45.6	400	0.495
15.0~32.6	18.05	0.50	45.6~89.6	400	0.495
32.6~51.0	18.74	0.57	89.6~152.8	400	0.495

*: s_u in each clay layer varies linearly

(b) Parameters for sand

Depth (m)	γ_t (kN/m^3)	K_0	ϕ' ($\circ$)	c' (kPa)	K	n	ν
51.0~67.0	19.62	0.41	36	0.0	5601	0.5	0.3

The structural materials in this study, including the concrete diaphragm walls, cross walls, buttress walls and concrete slabs used in the top-down construction method and temporary steel struts, were simulated by the linear elastic model. The shell element was used for diaphragm walls, cross walls and buttress walls while the beam element was used for temporary steel struts and the concrete slabs. For simplifying the analyses, the excavation sites are assumed symmetric with respect to the center lines of the width and length of the sites. Therefore, only about one-quarter of the excavation area was adopted for analysis. When planning the meshes, the boundary in the horizontal directions (x and y directions) were placed at a distance of four times the excavation depth behind the wall, and the boundary in the depth direction (z direction) was placed at rock. The boundary of the bottom was restrained from both the vertical and horizontal movements while the vertical boundaries were restrained from the horizontal movement.

3.2. Analysis results

Fig. 7 shows the comparison of the observed wall deflections and surface settlements at SI-8 (SET8) and SO-1 (SET1) sections at the final excavation stage and those computed from the analyses. The analyses follow the exact construction sequence and allocation of cross walls and buttress walls. In addition, analyses of the case with the assumption of no cross walls and buttress walls (w/o CW and BW) are performed, and the results are shown in the same figures.

Fig. 7 shows that the computed wall deflections for excavations without cross walls are quite consistent with the excavations in Taipei as studied by Ou (1993). The computed wall deflections for the studied case, i.e., the excavation with cross walls, were quite close to the observed though poor computation for surface settlement was obtained because the small strain behavior of the soil far from the diaphragm wall was not taken into account. As long as the lateral wall deflection was concerned, the adopted simulation of construction sequence, constitutive models and selection procedure of parameters in this study can be justified.
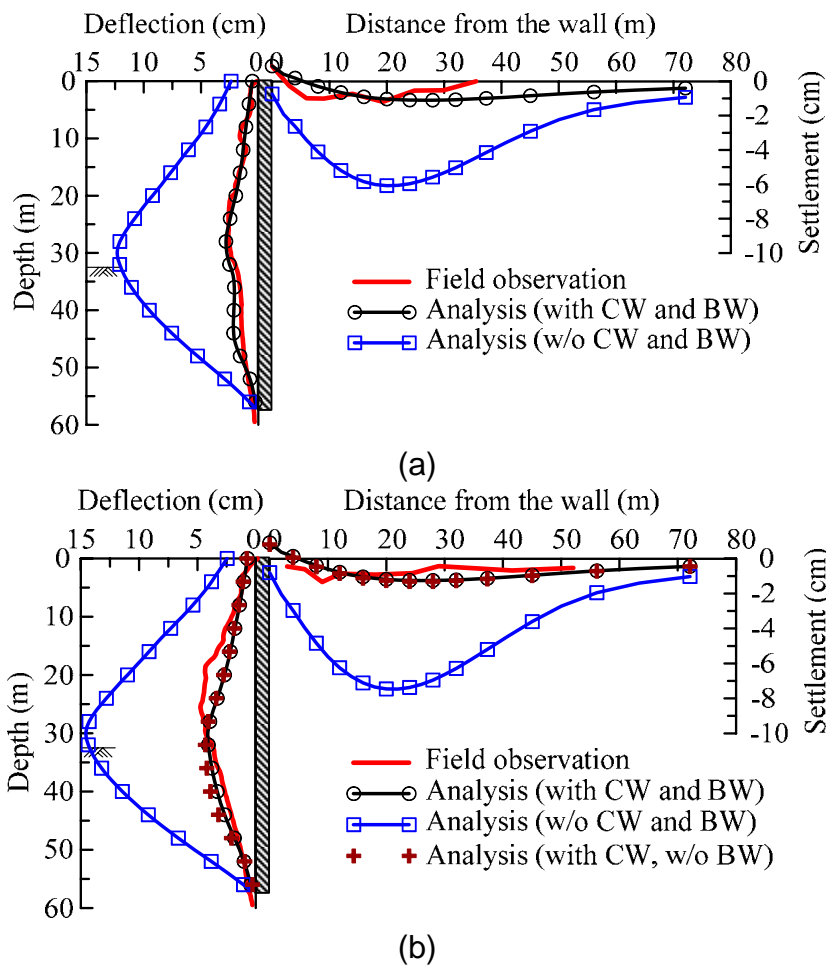
Fig. 7. Comparison of wall deflections and surface settlements from field observation and those from analysis at final excavation stage (a) SI-8 (SET8) and (b) SO-1 (SET1) sections.

Fig. 7(a) also shows that the computed wall deflections and surface settlements at the cross wall installed section, i.e., SI-8 (SET8), was much smaller than those without cross walls and buttress walls. Installation of cross walls can substantially reduce lateral wall deflections and surface settlements. The maximum wall deflection and surface settlement at the final excavation stage were reduced by 77% and 80%, respectively, by the installation of such walls. Like Fig. 7(a), Fig. 7(b) also shows that the computed wall deflections and surface settlements at the midpoint of two cross walls, i.e., SO-1(SET1) section, were much smaller than those without cross walls and buttress walls. Installation of cross walls and buttress walls can substantially reduce lateral wall deflections and surface settlements for the section at the midpoint between cross walls. The maximum wall deflection and surface settlement at the final excavation stage were reduced by 72% and 83%, respectively, by the installation of cross walls.

Furthermore, analysis of the excavation with only cross walls, i.e., no buttress walls, was carried out to examine the contribution of buttress walls at the midpoint of two cross walls, i.e., at SO-1(SET1) section, in reducing the lateral wall deflection and surface settlement. The computed results are also shown in Fig. 7(b). Little difference

between the case with cross walls and buttress walls and the case with only cross walls was found. Installation of additional buttress wall at the midpoint of two cross walls does not have any effect in further reducing the lateral wall deflection and surface settlement. Therefore, the effect of the buttress wall in reducing lateral wall deflections and surface settlements was insignificant.

4. PAREMETRIC STUDY

The influence of total depth of cross walls on the lateral wall deflection will be studied in terms of the cross wall height, referring to a measurement above the excavation surface (H_{ch}) and embedded cross wall, referring to a measurement below excavation surface (H_{ce}), as shown in Fig. 1. The concept of plane strain ratio proposed by Ou (1996) will be adopted to evaluate the effectiveness of cross walls on the lateral wall deflection. The plane strain ratio at the midpoint of two cross walls (PSR_C) were defined as

$$PSR_C = \frac{\delta_{hm,middle}}{\delta_{hm,ps}},$$

(2)

where $\delta_{hm,middle}$ is the maximum lateral wall deflection at the midpoint of two cross walls and $\delta_{hm,ps}$ is the maximum lateral wall deflection under the plane strain condition.
When designing cross walls, a smallest height ratio (H_{ch}/H_e) and embedment ratio (H_{ce}/H_p) should be adopted and meanwhile, its PSR_C should also be close to those with full height and full embedment, that is, H_{ch}/H_e =1 and H_{ce}/H_p =1. Therefore, the critical height ratio, (H_{ch}/H_e)$_{cr}$, is defined as the height ratio (H_{ch}/H_e) at which the resulting PSR_C was the same as that at H_{ch}/H_e =1 for a specific H_e, L', and B. Similarly, the critical embedment ratio, (H_{ce}/H_p)$_{cr}$, is defined as the embedment ratio (H_{ce}/H_p) at which the obtained PSR_C was the same as that at H_{ce}/H_p =1.
A basic assumed excavation was set up to perform parametric study to obtain (H_{ch}/H_e)$_{cr}$ and (H_{ce}/H_p)$_{cr}$ for various excavations. This assumed case was of the rectangular shape where the excavation width (B) was 40 m and excavation length (L) was infinite. The final excavation depth (H_e) was 20 m, which was completed in 7 stages. The temporary steel struts were installed at 1.0 m above the excavation surface and then excavation was conducted for the next stage of excavation. The diaphragm wall thickness was 1.0 m. The embedded diaphragm wall (H_p) was equal to H_e. The cross walls are with 20 m in interval (L') and 1.0m in thickness. The compressive strength (f'_c) of the diaphragm wall and cross wall was 27.5 MPa.
Moreover, the excavation was assumed to be in clay whose parameters were assumed the same as the third layer of above case history except the s_u was assumed to be equal to $0.3\sigma'_v$ where σ'_v was the effective vertical pressure. For parametric studies, the values of H_e, B, L', H_{ch} and H_{ce} were varied as shown in Table 2. Of them, $L' = \infty$ implies the excavation was not installed with cross walls and the wall deflection would be under the plane strain condition, in which the maximum lateral wall deflection was represented by $\delta_{hm,ps}$. This study performs the analysis of (H_{ch}/H_e)$_{cr}$ and (H_{ce}/H_p)$_{cr}$ for

the total of eight sets of excavations. The results are shown in Fig. 8. It is found that $(H_{ch}/H_e)_{cr}$ and $(H_{ce}/H_p)_{cr}$ were generally in the range of 0.4~0.6 and 0.5~0.7, respectively. Therefore, to have an economic design of a cross wall and also have a good reduction in wall deflection, it is reasonable to install the cross wall that both H_{ch}/H_e and H_{ce}/H_p are about equal to 0.6.

Table 2. Variation of the parameters in the parametric studies.

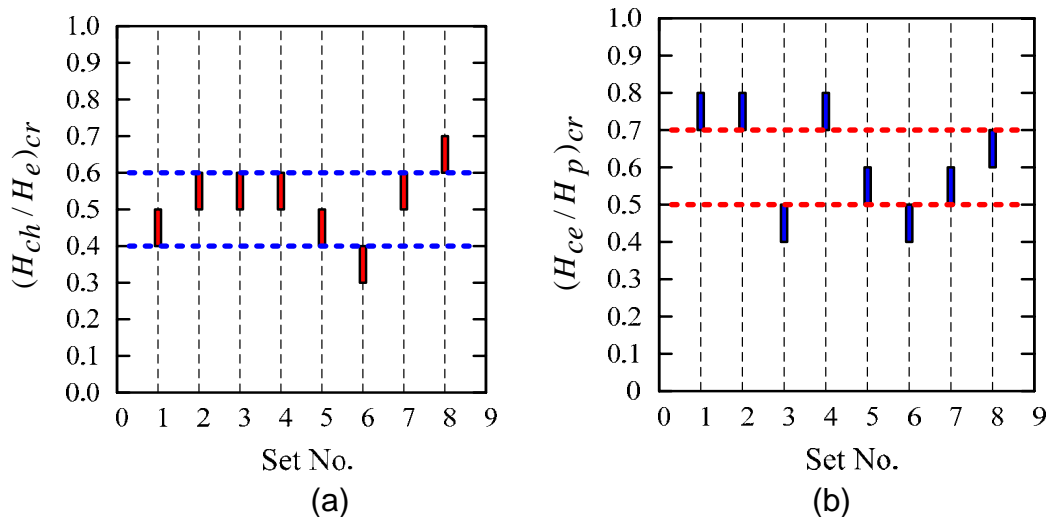| Parameters	Basic value	Variation
H_e (m)	20	10, 30
L' (m)	20	12, 28, 36, ∞^*
B (m)	40	20, 80
H_{ch} / H_e	1.0	0, 0.2, 0.4, 0.6, 0.8
H_{ce} / H_p	1.0	0, 0.2, 0.4, 0.6, 0.8

* : plane strain condition

Fig. 8. (a)Critical ratio of cross wall height for various sets of excavations (b)Critical ratio of cross wall embedment for various sets of excavations.

Fig. 9 shows the lateral wall deflections at the midpoint of two cross walls and at the cross wall section for the cases of H_{ch}/H_e =1.0, H_{ce}/H_p =1.0 and of H_{ch}/H_e =0.6, H_{ce}/H_p =0.6, when H_e =20 m, L' =28 m and B=40 m. For comparison, results from the analysis for no cross walls are also shown on the same figure. The lateral wall deflections for those with cross walls with different depths were all much smaller than those of no cross walls. Installation of cross walls obviously can reduce the lateral wall deflections at the midpoint of two cross walls and at the cross wall section. The figure also shows that an excavation with H_{ch}/H_e =1 and H_{ce}/H_p =1 can yield the best reduction in lateral wall deflections. The lateral wall deflections at the cross wall section and at the midpoint of the two cross walls for the case of H_{ch}/H_e =0.6, H_{ce}/H_p =0.6 are quite close to those with full cross wall height and embedment. Use of the cross wall height and

embedment at the critical condition can result in the same reduction in lateral wall deflections as the full cross wall height and embedment.
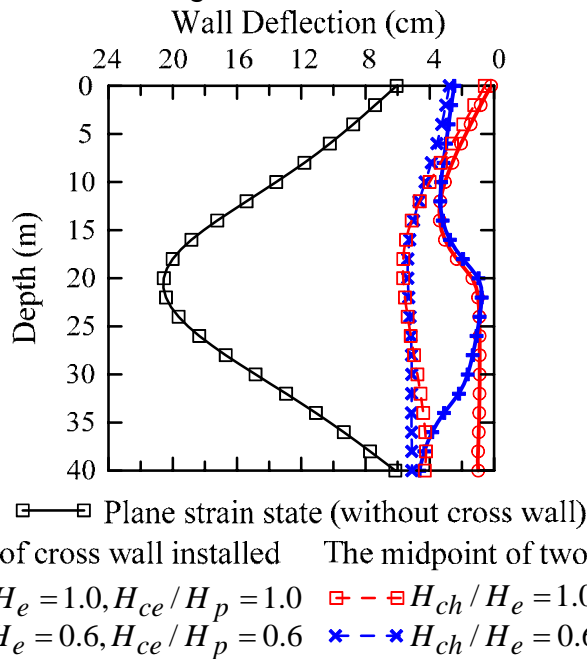

Fig. 9. Comparison of lateral wall deflections between the condition of critical wall height and embedment and full depth for H_e=20 m, L'=28 m and B=40 m.

CONCLUSION

Based on the study presented in this paper, the following conclusions can be drawn:
1. From the plane view, the lateral wall deflection increased with the increasing distance from the cross wall. Such behavior was similar to the three dimensional behavior of the diaphragm wall near the corner in an excavation. To realistic simulation of cross wall, a three dimensional numerical analysis is required.
2. The cross wall was effective in reducing the lateral wall deflection and ground settlement. The lateral wall deflection at the position where the cross wall was installed can be reduced to a very small amount. According to the case study, the maximum wall deflection and ground settlement compared to without cross walls and buttress walls was reduced by about 77% and 78% at the cross wall installed, respectively, and about 67% and 81% at the midpoint of two cross walls, respectively.
3. Use of the cross wall height of 0.4~0.6 times the excavation depth and cross wall embedment of 0.5~0.7 times the embedded diaphragm wall depth can yield the lateral wall deflection very close to that of full cross wall depth.

REFERENCES

Alpan, I. (1967). "The empirical evaluation of the coefficient $K0$ and $K0R$," Soils Found., Vol. **7**(1), 31-40.

Clough, G.W. and O'Rourke, T.D. (1990). "Construction-induced movements of in-situ walls," *Proc., Design and Performance of Earth Retaining Structure, ASCE Special Conf.*, ASCE, New York, 439-470.

Itasca Consulting Group, Inc. (1997) *FLAC3D: Fast Lagrangian Analysis of Continua 2.1*, Minn.

Jaky, J. (1944). "The coefficient of earth pressure at rest," J. Soc. Hungar. Archit. Eng. [in Hungarian], Vol. **78**(22), 355-358.

Janbu, N. (1963). "Soil compressibility as determined by oedometer and triaxial tests," *European Conf. on Soil Mechanics and Foundation Engineering*, Wiesbaden, Germany, Vol. **1**, 19-25.

Lim, A., Ou, C.Y. and Hsieh, P.G. (2010). "Evaluation of clay constitutive models for analysis of deep excavation under undrained conditions," *Journal of GeoEngineering*, Vol. **5**(1), 9-20.

Ou, C.Y., Chiou, D.C. and Wu, T.S. (1996). "Three dimensional finite element analysis of deep excavation," *J. Geotech. Eng.*, Vol. **122**(5), 337-345.

Ou, C.Y., Hsieh, P.G. and Chiou, D.C. (1993). "Characteristics of ground surface settlement during excavation," *Can. Geotech. J.*, Vol. **30**(5), 758-767.

Ou, C.Y., Hsieh, P.G. and Lin, Y.L. (2011). "Performance of excavations with cross walls," *J. Geotech. Geoenviron. Eng.*, Vol. **137**(1), 94-104.

Ou, C.Y. and Lai, C.H. (1994). "Finite-element analysis of deep excavation in layered sandy and clayey soil deposits," *Can. Geotech. J.*, Vol. **31**(2):204-214.

Ou, C.Y., Lin, Y.L. and Hsieh, P.G. (2006). "A case record of an excavation with cross walls and buttress walls," *Journal of GeoEngineering*, Vol. **1**(2), 579-86.